



Identification and prioritization of phytochemicals from medicinal plants with inhibitory activity against the transpeptidase enzyme of *Streptococcus pyogenes*

Zeynab Hejazi¹, Marzieh Etehadpour^{1*}, Mahboube Bagheri²

¹Department of Plan Production, Agriculture Faculty of Bardsir, Shahid Bahonar University of Kerman, Kerman, Iran.

²Department of Food Industrial, Agriculture Faculty of Bardsir, Shahid Bahonar University of Kerman, Kerman, Iran.

*Corresponding author,  0009-0007-2307-5282. Email: etehadpour@uk.ac.ir, m.etehtadpour@gmail.com.

ABSTRACT INFO

Research Paper

Received: 25 Jan 2025

Accepted: 28 May 2025

ABSTRACT

Antibiotic-resistant bacteria, particularly *Streptococcus pyogenes*, which is responsible for a wide array of diseases, represent a significant public health threat. Natural therapeutic agents derived from medicinal plants, notably essential oils, have garnered interest due to their potential antimicrobial properties. This study investigated the antibacterial activity of secondary metabolites from sixteen medicinal plants against *Streptococcus pyogenes* through bioinformatics approaches. A comprehensive insilico analysis was conducted on 890 phytochemicals to evaluate their interactions with the bacterial transpeptidase enzyme via molecular docking and molecular dynamics (MD) simulations. The transpeptidase enzyme sequence was subjected to various analytical procedures, including the ProtParam tool, EMBOSS Antigenic program, and VICMpred server. ProtParam analysis revealed that the enzyme has a molecular weight of 23.54 kDa, comprises 206 amino acids, with an isoelectric point (pI) of 6.24, an instability index of 31.21, and an aliphatic index of 83.25. The EMBOSS Antigenic program predicted eleven potential antigenic sites within the enzyme, with scores indicating cellular process involvement (1.1164), molecular information (-1.5058), molecular metabolism (-0.965), and virulence factors (-0.686). Molecular docking results identified that compounds from licorice, barberry, turmeric, plantain, nettle, cinnamon, aloe vera, and thyme exhibited significant binding affinities, with interaction energies ranging from -7.0 to -9.3 kcal/mol. Nineteen phytochemicals, including methoxyhydnicarpine, linalyl acetate, kaempferol, and glycyrrhizic acid, demonstrated high binding affinity and stability. MD simulations further confirmed that the enzyme-ligand complexes maintained considerable stability throughout the simulation duration. Additionally, the investigated molecules displayed favorable total interaction energies, spanning from -4.55507 to -90.562 kcal/mol. Collectively, these findings suggest that the identified natural compounds possess promising antibacterial potential, warranting further experimental validation and drug development efforts.

Key words: Medicinal plants, Molecular docking, Molecular dynamics, *Streptococcus pyogenes*, Transpeptidase.

How to cite this article:

Hejazi Z., Etehadpour M., and Bagheri M. (2025). Identification and prioritization of phytochemicals from medicinal plants with inhibitory activity against the transpeptidase enzyme of *Streptococcus pyogenes*. *Iranian Journal of Genetics and Plant Breeding*, 14(1): 9-24.

DOI: [10.30479/ijgp.2025.21425.1390](https://doi.org/10.30479/ijgp.2025.21425.1390)

©The Author(s).



Publisher: Imam Khomeini International University

IJGPB is an open access journal under the CC BY license (<http://creativecommons.org/licenses/by/4.0/>)

INTRODUCTION

Medicinal plants have historically served as a vital resource for drug discovery and development. Since ancient times, a diverse array of plant species has been utilized therapeutically in traditional medicine systems worldwide. Notable examples include garlic (*Allium sativum*), ginger (*Zingiber officinale*), cloves (*Syzygium aromaticum*), cardamom (*Elettaria cardamomum*), mint (*Mentha* spp.), and coriander (*Coriandrum sativum*). Contemporary research underscores the significance of plant-derived compounds, with nearly a quarter of drugs approved by the U.S. Food and Drug Administration (FDA) and the European Medicines Agency (EMA) originating from plant sources (Thomford *et al.*, 2018). These findings highlight the critical role of phytochemicals as a promising reservoir for novel therapeutic agents.

The rising prevalence of antimicrobial resistance (AMR), driven primarily by the overuse and misuse of antibiotics, has led to the emergence of multidrug-resistant (MDR) pathogens, posing an urgent global health challenge. This situation underscores the necessity of exploring alternative antimicrobial agents. Phytochemicals, characterized by their structural diversity and multi-target effects, interfere with essential cellular processes in pathogens, thereby offering a potentially effective strategy to combat AMR. For instance, Ashraf *et al.* (2023) identified 123 Himalayan medicinal plants containing bioactive phytochemicals with antimicrobial potential, emphasizing the importance of investigating plant-derived compounds as alternatives to synthetic antibiotics.

Despite their promise, significant challenges remain in the extraction, structural characterization, and clinical translation of phytochemicals. Critical steps such as establishing safety profiles, pharmacokinetics, and therapeutic efficacy must be addressed to facilitate their integration into clinical practice (Borkotoky and Banerjee, 2020). In this context, bioinformatics-based approaches—including molecular docking, molecular dynamics (MD) simulations, and quantitative structure-activity

relationship (QSAR) analyses—offer efficient, cost-effective tools for screening potential antimicrobial agents. Virtual screening accelerates drug discovery by identifying promising candidates within large chemical libraries, thereby reducing time and resource expenditures (Blundell *et al.*, 2006; Shakeran and Nosrati, 2019; Yırtıcı *et al.*, 2022).

Recent advances have increasingly recognized the vital role of bioinformatics in addressing persistent pathogens and complex diseases. For example, subtractive proteomics has facilitated the identification of novel drug targets in *Chlamydia pneumoniae*, a major causative agent of pneumonia and chronic conditions such as asthma. Through virtual screening of approximately 15,000 phytochemicals, coupled with molecular docking and MD simulations, researchers identified promising inhibitors targeting key bacterial proteins (Kadi *et al.*, 2022). Similarly, Islam *et al.* (2024) employed bioinformatics tools to screen 2,500 compounds derived from 25 medicinal plants for potential treatments of Alzheimer's disease (AD). Their analysis identified 80 candidates with favorable pharmacological properties, among which three compounds (CID 102267534, CID 15161648, and CID 12441) demonstrated strong binding affinity to acetylcholinesterase (AChE), supported by molecular docking, MD simulations, and density functional theory (DFT) calculations, suggesting their potential as AD therapeutics.

In the realm of infectious diseases, *Streptococcus pyogenes* (group A streptococcus), a Gram-positive pathogen, causes a spectrum of diseases ranging from mild infections to severe invasive conditions such as necrotizing fasciitis. It produces numerous virulence factors, including sortase—a cysteine transpeptidase critical for anchoring surface proteins involved in adhesion, immune evasion, and colonization. This enzyme, with the PDB ID 3PSQ, facilitates the attachment of surface proteins to the bacterial cell wall and plays a pivotal role in pathogenicity and persistence (Kang *et al.*, 2011). If left untreated, infections with *S. pyogenes* can lead to serious post-infectious complications, including rheumatic fever

and glomerulonephritis, with potential long-term health consequences (Guilherme *et al.*, 2006).

The current study aims to investigate the binding interactions of 890 compounds derived from 16 medicinal plants with the active site of *S. pyogenes* sortase. Specifically, molecular docking and MD simulations will be employed to identify potential inhibitors that demonstrate strong binding affinity and stable interactions within the enzyme's active site, thereby contributing to the search for novel antimicrobial agents targeting *S. pyogenes*.

MATERIALS AND METHODS

Collecting primary data

To facilitate molecular binding analyses, the three-dimensional structures of 890 phytochemical compounds derived from 16 medicinal plant species—including thyme (*Thymus vulgaris*), aloe vera (*Aloe barbadensis*), clove (*Syzygium aromaticum*), plantain (*Plantago major*), cinnamon (*Cinnamomum verum*), barberry (*Berberis vulgaris*), eucalyptus (*Eucalyptus globulus*), ginger (*Zingiber officinale*), hyssop (*Hyssopus officinalis*), sage (*Salvia officinalis*), nettle (*Urtica dioica*), turmeric (*Curcuma longa*), licorice (*Glycyrrhiza glabra*), violet (*Viola odorata*), oregano (*Origanum vulgare*), and mangrove (*Rhizophora spp.*)—were retrieved from the PubChem (<https://pubchem.ncbi.nlm.nih.gov/>) and DrugBank (<https://go.drugbank.com/>) databases. All structures were downloaded in Structure Data File (SDF) format.

The primary structure of the cysteine transpeptidase sortase enzyme (PDB ID: 3PSQ) was obtained from the Protein Data Bank (<https://www.rcsb.org/>). Both the ligands and the target protein were subsequently prepared for molecular docking analyses using DS Visualizer, UCSF Chimera, and AutoDockTools software.

The crystal structure of 3PSQ (Spy0129/SrtC1 from *Streptococcus pyogenes*) was selected based on the following key considerations:

- **Critical role in bacterial virulence and pilus assembly**

SrtC1 is a class B sortase enzyme that mediates the covalent linkage of pilin subunits within *S. pyogenes* pili, which are crucial in bacterial adhesion, colonization, and pathogenicity. Unlike the housekeeping sortase SrtA, SrtC1 specifically facilitates pilus biogenesis, rendering it an attractive target for antimicrobial strategies aimed at impairing bacterial infectivity (Kang *et al.*, 2011).

- **Pathogen-specific therapeutic potential**

Streptococcus pyogenes is a clinically important pathogen, and sortases are absent in human hosts, thus minimizing potential off-target effects in drug development (Mangal *et al.*, 2023). Prior computational investigations, including docking and MD simulations targeting *S. pyogenes* SrtC, have demonstrated the viability of using sortase enzymes as targets in virtual screening approaches—further supporting their relevance in this study involving phytochemicals from 16 plant species.

Transpeptidase enzyme sequence analysis

The amino acid sequence of the transpeptidase enzyme from *Streptococcus pyogenes* (PDB ID: 3PSQ) was obtained from the UniProt protein sequence database (<https://www.uniprot.org/>). Key physicochemical properties of the enzyme were calculated using the ProtParam tool (<https://web.expasy.org/protparam/>), including amino acid composition, molecular weight (MW), theoretical isoelectric point (pI), instability index (II), and aliphatic index (AI). Additionally, potential antigenic determinants were predicted using the EMBOSS Antigenic server (https://www.bioinformatics.nl/cgi-bin/emboss/antigenic?_pref_hide_optional=1). To further characterize the protein, the VICMpred server (<https://webs.iitd.edu.in/raghava/vicmpred/help.html>) was employed to predict its functional class, providing insights into the nature and role of the enzyme.

Preparation of ligands and protein for docking

The preparation of ligands and the target protein for molecular docking was conducted through a series of meticulous steps to ensure accuracy and reproducibility. Initially, cofactors and water molecules were removed from the protein and ligand structures using Visualizer 5.3 (Hanwell *et al.*, 2012). Subsequently, all ligands and receptor molecules underwent three-dimensional structure optimization using UCSF Chimera (Pettersen *et al.*, 2004), with the aim of obtaining the most stable conformations with minimized energy.

Ligand preparation for docking was performed using AutoDockTools (Morris *et al.*, 2009). This process involved calculating Gasteiger-Marsili partial charges, adding hydrogens (including non-ionized hydrogens), and defining rotatable bonds and the centroid of each ligand molecule. Further energy minimization, hydrogen addition, and torsion adjustments were carried out, with the finalized structures saved in pdbqt format.

The protein structure was prepared in a similar manner with AutoDockTools. Hydrogens were added,

and the molecule's total charge was assigned using the Kollman united-atom charge scheme. Non-ionized hydrogens were added to appropriate carbon atoms, and non-essential parts were removed prior to docking setup. The finalized protein structure was converted into pdbqt format for subsequent docking procedures with AutoDock Vina (Trott and Olson, 2010).

To define the binding site, the CASTp server (<http://sts.bioe.uic.edu/castp/index.html>) was employed to identify potential cavities, and PyMOL was used to visualize and precisely determine the binding site center for docking simulations. All docking computations employed an iterative local search optimization algorithm, treating the protein as a rigid receptor and the ligands as flexible entities.

Molecular docking analysis

Molecular docking was performed using AutoDock Vina to predict the binding conformations and affinities of ligands within the active sites of the target proteins. The resulting ligand-receptor complexes, including binding poses, orientations, and interaction energies, were visualized and analyzed using BIOVIA Discovery Studio (version 2020). To further characterize the specific molecular interactions—such as hydrogen bonding and hydrophobic contacts—LigPlot+ v.2.2.5 was employed, enabling the identification of key amino acid residues involved in ligand binding and stabilization.

Molecular dynamics simulation

Compounds exhibiting high binding affinity from molecular docking analyses were subjected to further molecular dynamics (MD) simulations to evaluate their stability and interaction profiles over time. Simulations were performed using GROMACS 2020 on a Linux operating system.

Ligand topologies were generated via the CHARMM General Force Field (CGenFF) server, which requires input structures in Sybyl. mol2 format to obtain atomic types and bond connectivity parameters. CGenFF provides an all-atom force field that explicitly represents hydrogen atoms, which are often absent in crystal structures, thereby ensuring accurate modeling of ligand interactions. The Avogadro software was employed to generate the mol2 files and incorporate missing hydrogen atoms. The protein topology was constructed using the pdb2gmx utility within GROMACS.

The CHARMM36 force field, downloaded from the MacKerell laboratory's repository, was used for all simulations. The topology files encompass

parameters for bonds, angles, torsions, and non-bonded interactions. Bond potentials account for interactions between chemically bonded atoms, angle potentials describe interactions involving three atoms, and dihedral (torsion) potentials involve four atoms, collectively defining the conformational energy landscape.

Non-bonded interactions were modeled to include electrostatic and van der Waals forces. Van der Waals interactions were described via the Lennard-Jones potential, while electrostatic interactions followed Coulomb's law. For atom pairs with partial charges q_i and q_j , separated by distance r_{ij} , the electrostatic interaction energy is given by:

$$(1) \quad \text{Electrostatic} = \sum \frac{q_i q_j}{\epsilon r_{ij}}$$

Where: ϵ is the dielectric constant.

The van der Waals interactions are represented by:

$$(2) \quad E_{vdW} = \sum \frac{A_{ij}}{r_{ij}^{12}} - \frac{B_{ij}}{r_{ij}^6}$$

Following topology generation, the simulation system was assembled by defining the simulation box with a minimum distance of 1 nm between the solute (protein-ligand complex) and the box boundary. Solvent molecules—typically TIP3P water—were added to solvated the system, ensuring a realistic environment and system stability (Figure 1). To neutralize the overall charge, counterions were incorporated: chloride ions (Cl⁻) were added for positively charged molecules, and sodium ions (Na⁺) for negatively charged molecules, replacing some water molecules.

The next steps involved generating the input run parameters: a .tpr file was created via the grompp command, followed by the addition of ions through the genion utility to neutralize the system. Energy minimization was then performed using the steepest descent algorithm, executing 50,000 steps until reaching a convergence tolerance of 1,000 kJ/mol·nm.

Long-range electrostatic interactions were computed using the Particle Mesh Ewald (PME) method with a real-space cutoff of 1.2 nm and a Fourier grid spacing of 0.16 nm. Equilibration protocols included: (1) NVT ensemble at 310 K for 1 ns with a 0.1 ps time step, maintaining temperature via the velocity-rescaling thermostat; and (2) NPT ensemble at 1 bar with Parrinello-Rahman pressure coupling, a compressibility of $4.5 \times 10^{-5} \text{ bar}^{-1}$, and a coupling constant of 2 ps, also for 1 ns.

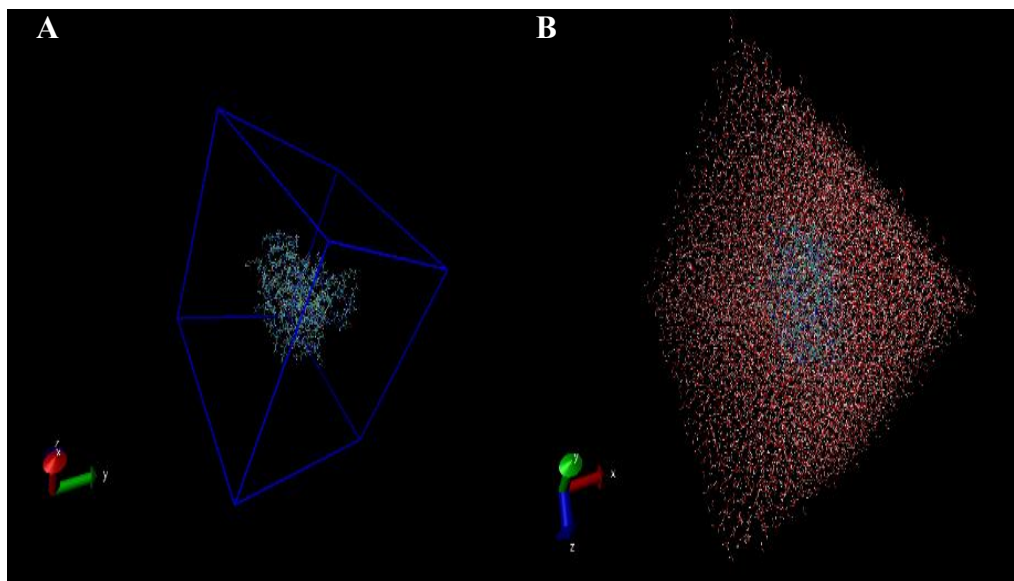


Figure 1. The steps of creating **A:** the simulation box and **B:** solvent coating of Gromax molecular simulation.

Subsequently, production MD simulations were conducted over 100 ns with an integration time step of 2 fs, employing the LINCS algorithm (Hess *et al.*, 1997) to constrain all bonds involving hydrogen atoms. The stability and conformational behavior of the protein-ligand complexes were analyzed using GROMACS's internal analysis tools. Trajectory data were visualized using Visual Molecular Dynamics (VMD) and Grace Software for comprehensive assessment.

Validation of docking results

The stability of the selected protein-ligand complexes was evaluated by calculating the RMSD of atomic positions over the course of MD simulations, providing insights into the binding stability and conformational integrity of the complexes.

RESULTS AND DISCUSSION

Transpeptidase enzyme sequence analysis

The amino acid sequence of the transpeptidase enzyme was obtained from the UniProt protein sequence database. Physicochemical properties were computed using ProtParam, revealing a molecular weight of 23.54 kDa, an amino acid length of 206 residues, a theoretical isoelectric point (pI) of 6.24, an instability index of 31.21, and an aliphatic index of 83.25. These parameters suggest that the enzyme is thermodynamically stable under physiological conditions. Additionally, the EMBOSS Antigenic program predicted eleven potential antigenic sites, which may be involved in protein-ligand interactions during molecular docking and molecular

dynamics simulations.

Further functional insights were obtained using the VICMpred server, which predicted the enzyme's involvement in cellular processes with a score of 1.1164, molecular information at -1.5058, molecular metabolism at -0.965, and virulence factors at -0.686. This analysis indicates that the protein likely exhibits virulence-associated characteristics. VICMpred employs support vector machine (SVM) algorithms that analyze patterns based on amino acid and dipeptide composition, achieving an overall accuracy of approximately 75%.

A summary of the sequence-based properties of the transpeptidase enzyme is presented in Table 1. Additionally, Verify3D scores for the 3PSQ structure are depicted in Figure 2. Notably, fewer than 80% of the amino acids scored ≥ 0.1 in the 3D/1D profile, indicating potential regions of structural inconsistency or areas warranting further validation.

Molecular docking

Docking calculations were conducted using AutoDock Vina to evaluate the interaction of 890 plant-derived compounds with the cysteine transpeptidase enzyme from *Streptococcus pyogenes*. Binding affinities were expressed in kcal/mol. The results are summarized in Table 2. The binding energies of the studied compounds ranged from -2.2 to -9.3 kcal/mol, with more negative values indicating stronger binding affinity between the enzyme (receptor) and the inhibitor (compound).

Table 1. Predicted structural and functional properties of the transpeptidase enzyme.

Tools	Description	Obtained results
ProtParam	Calculation of various physicochemical properties	Molecular weight (23.54 kDa), amino acid length (206), theoretical isoelectric point (pI) (6.24), instability index (31.21), aliphatic index (83.25)
EMBOSS –antigenic	Finding possible antigenic sites in the protein sequence	11 antigenic sites
VICM pred	Classification of bacterial proteins into cellular process, molecular information, molecular metabolism and pathogenic factors	Cell process (1.1164), molecule information (-1.5058), molecule metabolism (-0.965), pathogenic factors (-0.686)

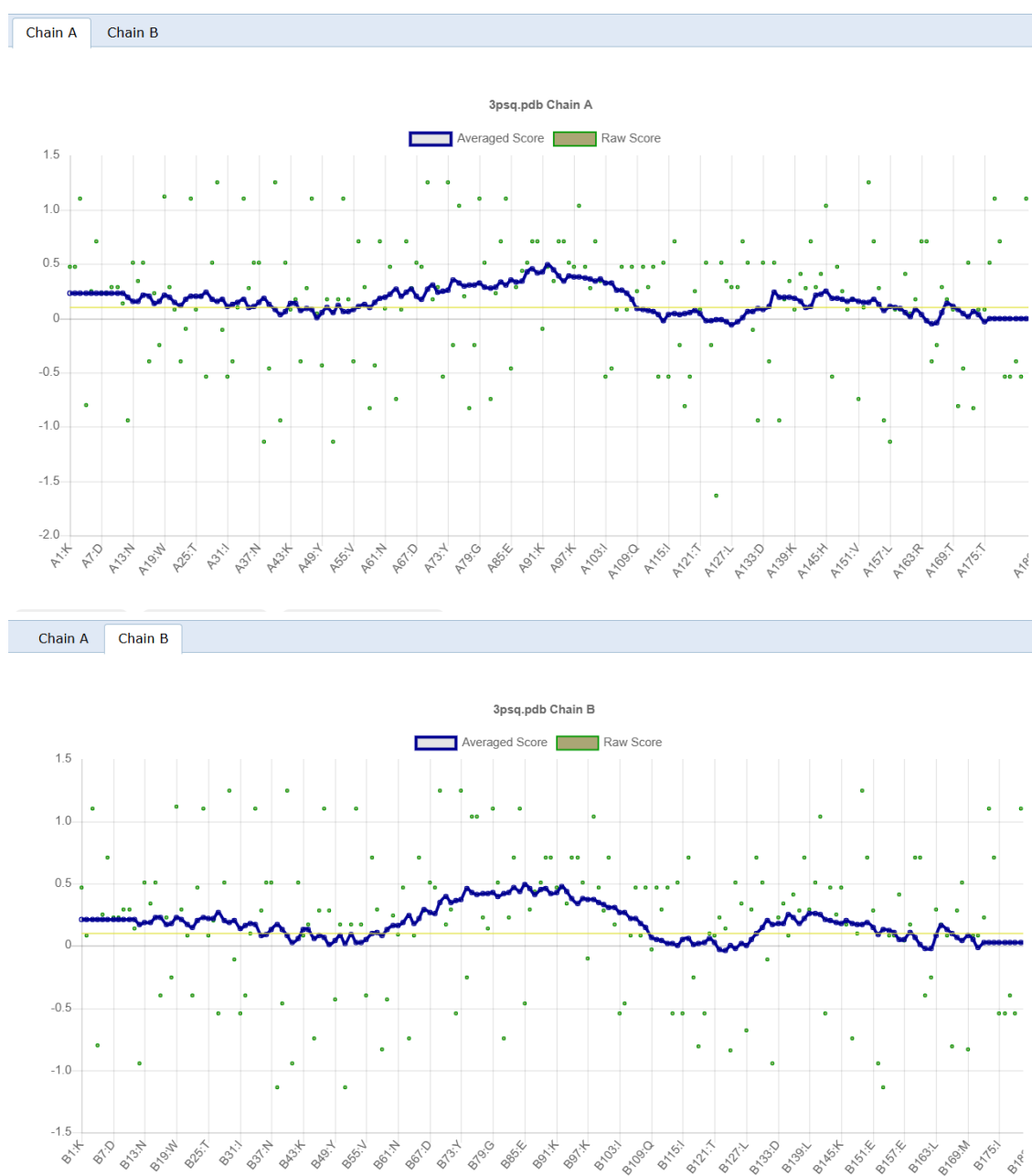


Figure 2. Verify3D scores for the 3PSQ structure.

Table 2. Analysis of molecules binding of selected compounds.

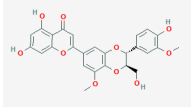
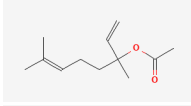
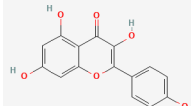
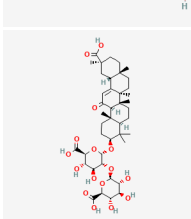
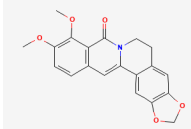
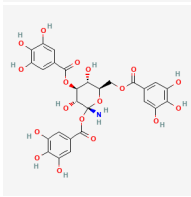
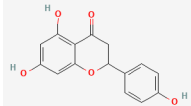
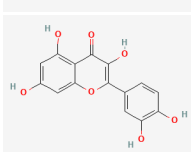
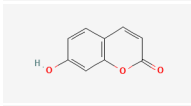
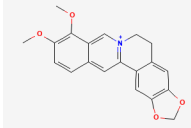
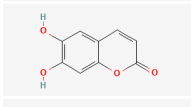
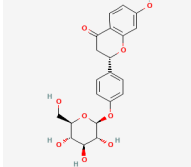
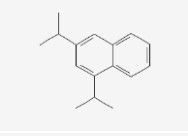
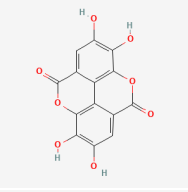
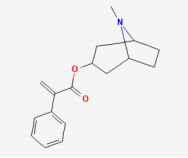
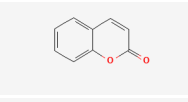
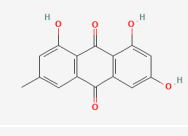
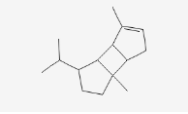
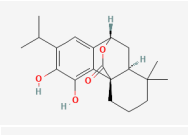
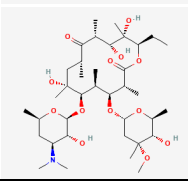
Compound name	Plant	Pubchem ID	Molecular formula	Chemical scheme	Docking score (-)
5'-methoxyhydrnocarpin	Licorice	5281879	C ₂₆ H ₂₂ O ₁₀		9.3
Linalyl acetate	Plantain	8294	C ₁₂ H ₂₀ O ₂		9
Kaempferol	Licorice	5280863	C ₁₅ H ₁₀ O ₆		8.4
Glycyrrhizic acid	Licorice	14982	C ₄₂ H ₆₂ O ₁₆		8
Berberine	Barberry	11066	C ₂₀ H ₁₇ NO ₅		7.9
Tannin	Barberry	129693153	C ₂₇ H ₂₅ NO ₁₈		7.8
Naringenin	Licorice	932	C ₁₅ H ₁₂ O ₅		7.7
Quercetin	Turmeric and plantain	5280343	C ₁₅ H ₁₀ O ₇		7.6
Umbelliferone	Turmeric	5281426	C ₉ H ₆ O ₃		7.4
Berberine	Barberry	2353	C ₂₀ H ₁₈ NO ₄ ⁺		7.4
Esculetin	Barberry	5281416	C ₉ H ₆ O ₄		7.4
Liquiritin	Licorice	503737	C ₂₁ H ₂₂ O ₉		7.4

Table 2 (Continued). Analysis of molecules binding of selected compounds.

Compound name	Plant	Pubchem ID	Molecular formula	Chemical scheme	Docking score (-)
1,3-diisopropyl-naphthalene	Plantain	92672	C ₁₆ H ₂₀		7.3
Ellagic acid	Turmeric	5281855	C ₁₄ H ₆ O ₈		7.3
Apoatropine	Nettle	64695	C ₁₇ H ₂₁ NO ₂		7.3
Coumarin	Cinnamon	323	C ₉ H ₆ O ₂		7.3
Emodin	Aloe vera	3220	C ₁₅ H ₁₀ O ₅		7.3
Alpha-bourbonene	Thyme	530816	C ₁₅ H ₂₄		7.2
Carnosol	Turmeric	442009	C ₂₀ H ₂₆ O ₄		7.2
Kanamycin	-	6032	C ₁₈ H ₃₆ N ₄ O ₁₁		7.3
Erythromycin	-	12560	C ₃₇ H ₆₇ NO ₁₃		6.2

Comparative analysis of the interactions revealed that compounds from licorice, barberry, turmeric, plantain, nettle, cinnamon, aloe vera, and thyme exhibited the strongest interactions, with binding energies between -7 and -9.3 kcal/mol. Conversely, compounds from oregano, eucalyptus, sage, hyssop, and mangrove displayed comparatively weaker interactions, with binding energies ranging from -6 to -7 kcal/mol. Among these, the mangrove-derived

compounds showed the weakest interactions, with energies between -4 and -7.3 kcal/mol.

Notably, specific compounds demonstrated minimal binding affinity: acetaldehyde from cinnamon (-2.2 kcal/mol), methyl myristate from plantain (-2.8 kcal/mol), propanoate from thyme (-3.2 kcal/mol), isovaleric aldehyde from cinnamon (-3.6 kcal/mol), and n-caproaldehyde from mangrove (-3.7 kcal/mol). These exhibited the lowest binding affinities and, thus,

the least potential for effective inhibition of the *S. pyogenes* transpeptidase enzyme.

Analyzing the amino acids involved in hydrophobic and hydrogen bond formation using LigPlot+ software revealed key interactions. As depicted in Figure 3, quercetin formed hydrogen bonds with cysteine 13 (Cys13A), aspartic acid 115 (Asp115A), and isoleucine 12 (Ile12A), indicated by green dashed lines. Hydrophobic interactions involved amino acids such as Gly10A, Trp117A, Trp41A, Cys8A, Leu9A, and Glu42A. A ball-and-stick model visually represented the ligand within the active site, illustrating these interactions.

Considering the resource-intensive nature of laboratory screening for herbal compounds, bioinformatics tools have emerged as impactful adjuncts, offering significant time and cost efficiencies. Recent studies highlight the antibacterial potential of secondary metabolites from medicinal plants against *S. pyogenes*. This study further evaluates the interaction and inhibitory potential of selected plant compounds against the *S. pyogenes* transpeptidase enzyme using molecular docking and molecular dynamics approaches. *S. pyogenes* is a prevalent human pathogen responsible for a spectrum of conditions, from mild infections like pharyngitis and impetigo to severe diseases such as necrotizing fasciitis, sepsis, and toxic shock syndrome (Piard *et al.*, 1997).

The present findings indicate that most of the investigated compounds exhibit notable in silico inhibitory potential against the 3PSQ enzyme, with binding energies ranging from -2.2 to -9.3 kcal/mol. Nineteen compounds—namely methoxyhydrnocarpine, linalylacetate, kaempferol, glycyrrhizic acid, berlambin, tannin, naringenin, quercetin, amblyferon, berberine, askoltin, liquiritin, 1,3-dipropynyl naphthalene, ellagic acid, apotropin, coumarin, emodin, alpha-bourbonene, and carnosol—derived from licorice, plantain, barberry, turmeric, nettle, cinnamon, aloe vera, and thyme, demonstrated the strongest affinity for the transpeptidase enzyme. Kanamycin and erythromycin served as reference antibiotics; the former generally exhibited the lowest docking scores among the plant compounds, while erythromycin consistently showed the strongest binding across all tested compounds.

Aligning with findings by Barh *et al.* (2011), who identified ten leading non-herbal pharmaceutical inhibitors targeting apoptosis-related enzymes, these results suggest that the highlighted herbal compounds could serve as potential inhibitors of the *S.*

pyogenes transpeptidase enzyme, warranting further exploration of their therapeutic potential.

Supporting this, Shakeran and Nosrati (2019) investigated plant compounds from *Ferulago angulata*, *Laurus nobilis*, and *Scrophularia striata* concerning antibiotic resistance proteins in *Staphylococcus aureus*. Their analysis revealed effective interactions, notably with VanX, with palmitic acid and bis (2-ethylhexyl) phthalate demonstrating the strongest affinities. Bis (2-ethylhexyl) phthalate, derived from *S. striata*, exhibited high interaction energies with PBP2 and β -lactamase, enzymes crucial for bacterial cell wall synthesis and antibiotic resistance, with laboratory studies validating their antibacterial activities. Palmitic acid showed the highest interaction energy with VanA, suggesting that these compounds could impede their target protein activities, positioning them as promising candidates for further experimental validation (Shakeran and Nosrati, 2019).

Additionally, research on the antiviral effects of *Ruellia tuberosa* and *Ruellia patula* identified key metabolites, including catechin, gallic acid, rutin, and chlorogenic acid, via LC-MS/MS and HPLC. The antiviral activity was assessed against HAdV-40, HSV-2, and H1N1 viruses. *Ruellia tuberosa* demonstrated stronger antiviral effects against most viruses, with *R. patula* particularly effective against HSV-2. Molecular docking and dynamics studies confirmed stable interactions between these bioactive compounds and viral targets, underscoring their potential as alternative antiviral agents (Melk and Sayed, 2024).

Complementing this, Mangal *et al.* (2023) identified three promising inhibitors (CID: 13888122, CID: 3694932, and CID: 102445430) targeting Sortase C, a key enzyme involved in *S. pyogenes* cell wall biosynthesis. Using an integrated computational pipeline—including protein modeling, virtual screening, and molecular dynamics—they demonstrated stable binding and favorable drug-like properties, suggesting potential for further preclinical development.

Similarly, Rehman *et al.* (2021) employed a subtractive proteomics approach to identify novel drug targets in *S. pyogenes*. Narrowing down to 145 non-human homologs, they identified DnaA and a two-component response regulator as promising cytoplasmic targets. Screening over 1000 phytochemicals via docking and simulation revealed a lead compound with potential antibacterial activity.

Finally, a study on *Murraya koenigii* (curry leaf)

identified several bioactives, including O-methyl murrayamine, koenigine, koenigicine, and murrayone, with notable inhibitory effects against *Streptococcus mutans*, a pathogen responsible for dental caries. Notably, molecular docking revealed koenigicine as the strongest binder, indicating its potential application in oral health products such as antibacterial toothpaste (Maheswari and Sankar, 2024).

Prediction of physicochemical properties and toxicity potential of the studied compounds

The physicochemical and pharmacokinetic properties of the hit compounds, identified through docking studies, were evaluated using pkCSM. The parameters assessed include Lipinski's rule of five, compound solubility, and additional pharmacokinetic factors (Table 3).

Molecular dynamics simulation results

Compounds with high docking scores were further evaluated through molecular dynamics (MD) simulations. To assess the stability of the system, fluctuations in physical quantities such as temperature, kinetic energy, potential energy, and total energy were examined over time. A stable system is characterized by fluctuations around a constant mean value.

System equilibrium was demonstrated by analyzing the trajectories of temperature and energy changes as functions of simulation time. As shown in Figure 4A, temperature fluctuations remained minimal throughout the simulation, indicating thermal stability. The potential energy of the system was obtained by averaging over time, considering all pairwise interactions between force centers; this parameter was calculated at each simulation step. As depicted in Figures 4B and 4C, both the average potential and total energies remained nearly constant during the NPT simulation intervals, further confirming the system's equilibrium.

The final phase of the analysis involved trajectory examination to evaluate the overall flexibility and stability of the protein, focusing on parameters such as root mean square deviation (RMSD), radius of gyration, and energy. RMSD is a critical indicator of model stability, reflecting how much the atomic positions deviate from their initial reference over time. A higher RMSD denotes greater structural change, whereas a lower RMSD or a slope approaching zero suggests enhanced stability. Conversely, increasing or fluctuating RMSD indicates instability within the model (Carugo and Pongor, 2001). Figure 4D illustrates the RMSD trajectories, reflecting the model's stability throughout the simulation.

Since direct measurement of individual atom distances from the protein's center of mass is not feasible, the radius of gyration is employed as an alternative metric. This parameter assesses whether the protein maintains its folded state; smaller values indicate a more compact, folded structure, while larger values suggest unfolding or extension. As shown in Figure 4E, the radius of gyration remained relatively constant during the simulation, indicating that the protein retained its structural stability throughout the process.

Interaction energies

The total protein-ligand interaction energy was calculated as the sum of van der Waals and electrostatic energies, as detailed in Table 4. All selected compounds exhibited relatively low total interaction energies, indicating favorable interactions with the target protein. These findings support the potential of the investigated compounds as effective enzyme inhibitors.

Molecular dynamics (MD) simulation is a computational approach based on Newton's equations of motion and principles of statistical mechanics. It enables the modeling of atomic and molecular movements and interactions, providing valuable insights into the dynamic behavior of biological systems. During MD simulations, atoms and molecules interact according to physical laws over specified timeframes, allowing the analysis of their trajectories and interactions. This method permits the *in silico* testing of materials without the need for laboratory synthesis (Nair and Miners, 2014). By solving the equations of motion over time, MD explores the relationships between molecular structure, dynamics, and function, facilitating the prediction of macroscopic properties from microscopic data—properties that are often challenging to measure directly (Nair and Miners, 2014; Hospital *et al.*, 2015).

MD simulations are particularly valuable for studying materials under extreme conditions and for predicting the behavior of macromolecules within various environments. Comparing simulation results with experimental data helps validate or challenge existing theoretical models (Nair and Miners, 2014). The simulation process typically involves three main steps: (a) Model Building—constructing a computational model of the system; (b) Trajectory Calculation—determining the positions and velocities of molecules over time; and (c) Trajectory Analysis—examining the generated trajectories to understand molecular behavior. The trajectory calculation step is especially critical, as it involves using equations of motion to monitor atomic and molecular positions dynamically (Groenhof, 2013).

Table 3. Pharmacokinetic properties of the top candidates against transpeptidase enzyme.

Standard parameters	5'-Methoxyhydroxycarpin	Linalyl acetate	Kaempferol	Glycyrrhizic acid	Berlambine	Tannin	Naringenin	Quercetin	Umbelliferone	Berberine	Esculetin	Liquiritin	1,3-diisopropyl-naphthalene	Ellagic acid	Apoatropine	Coumarin	Emodin	Alpha-bourbonene	Carnosol
Water solubility (log mol/L)	-3.1	-3.1	-3.0	-2.8	-4.2	-2.8	-3.2	-2.9	-2.1	-3.9	-2.4	-3.3	-6.0	-3.1	-2.7	-1.5	-3.1	-5.9	-4.1
Caco2 permeability (log Papp. In 10 ⁶ cm/s)	0.3	1.6	0.0	-0.7	1.0	-2.3	1.0	-0.2	1.2	1.7	0.3	0.5	1.4	0.3	1.6	1.6	0.0	1.3	0.5
Intestinal absorption (human) (% Absorbed)	94.7	95.2	74.2	0	100	0	91.3	77.2	94.5	97.1	86.2	46.0	94.4	86.6	95.5	97.3	74.4	95.7	91.2
Skin Permeability (log Kp)	-2.7	-1.9	-2.7	-2.7	-2.6	-2.7	-2.7	-2.7	-2.6	-2.5	-2.7	-2.7	-2.4	-2.7	-2.9	-1.9	-2.7	-2.0	-2.8
P-glycoprotein substrate	✓	x	✓	✓	x	✓	✓	x	x	✓	✓	✓	✓	✓	x	x	✓	x	✓
P-glycoprotein I inhibitor	✓	x	x	x	✓	x	x	x	x	x	x	x	x	x	x	x	x	x	✓
P-glycoprotein II inhibitor	✓	x	x	x	✓	x	x	x	✓	✓	x	x	x	x	x	x	x	x	x
VDss (human) (log L/kg)	-0.4	0.0	1.2	-0.5	-0.0	0.6	-0.0	1.5	0.0	0.5	0.5	-0.1	1.1	0.3	0.9	-0.1	0.4	0.7	0.8
Fraction unbound (human) (Fu)	0.0	0.4	0.1	0.4	0.1	0.3	0.0	0.2	0.4	0.2	0.4	0.1	0	0.0	0.3	0.3	0.1	0.1	0.0
BBB permeability (log BB)	-1.4	0.5	-0.9	-1.5	-0.0	-3.4	-0.5	-1.0	-0.2	0.1	0.0	-1.1	0.6	-1.2	0.2	-0.0	-0.7	0.8	-0.0
CNS permeability (log PS)	-3.8	-2.3	-2.2	-4.3	-2.1	-5.3	-2.2	-3.0	-2.7	-1.5	-2.2	-3.8	-0.9	-3.5	-2.5	-1.9	-2.3	-1.5	-1.8
CYP2D6 substrate	x	x	x	x	x	x	x	x	x	x	x	x	x	x	x	x	x	x	x
CYP3A4 substrate	✓	x	x	x	✓	x	x	x	x	✓	x	x	✓	x	✓	x	x	✓	✓
CYP1A2 inhibitor	x	x	✓	x	✓	x	✓	✓	✓	✓	x	x	✓	x	x	✓	✓	x	x
CYP2C19 inhibitor	x	x	x	x	✓	x	x	x	x	x	x	x	✓	x	x	x	x	x	✓
CYP2C9 inhibitor	✓	x	x	x	✓	x	x	x	x	x	x	x	✓	x	x	x	x	x	x
CYP2D6 inhibitor	x	x	x	x	x	x	x	x	x	x	x	x	x	x	✓	x	x	x	x
CYP3A4 inhibitor	✓	x	x	x	✓	x	x	x	✓	x	x	x	✓	x	x	x	x	x	x

Table 3 (Continued). Pharmacokinetic properties of the top candidates against transpeptidase enzyme.

Standard parameters	5'-Methoxyhydrocarpin	Linalyl acetate	Kaempferol	Glycyrrhizic acid	Berlambine	Tannin	Naringenin	Quercetin	Umbelliferone	Berberine	Esculetin	Liquiritin	1,3-diisopropyl-naphthalene	Ellagic acid	Apoatropine	Coumarin	Emodin	Alpha-bourbonene	Carnosol
Total Clearance (log ml/min/kg)	0.2	1.6	0.4	-0.3	0.1	-0.2	0.0	0.4	0.7	1.2	0.6	0.3	0.1	0.5	0.9	0.9	0.3	0.9	0.2
Max. tolerated dose (human) (log mg/kg/day)	0.5	0.5	0.5	0.3	-0.2	0.4	-0.1	0.4	0.6	0.1	-0.2	0.1	0.6	0.4	0.1	0.4	0.1	-0.3	0.2
hERG I inhibitor	x	x	x	x	x	x	x	x	x	x	x	x	x	x	x	x	x	x	x
hERG II inhibitor	✓	x	x	x	x	✓	x	x	x	x	x	x	x	x	x	x	x	x	x
Oral Rat Acute Toxicity (LD50) (mol/kg)	2.6	1.7	2.4	2.4	2.3	2.4	1.7	2.4	2.0	2.5	2.3	2.5	2.2	2.3	2.6	2.1	2.1	1.5	2.1
Oral Rat Chronic Toxicity (LOAEL) (log mg/kg_bw/day)	2.1	2.2	2.5	3.0	2.2	6.6	1.9	2.6	1.7	1.8	1.5	3.7	1.3	2.6	1.5	1.9	2.0	1.3	1.9
Hepatotoxicity	x	x	x	x	✓	x	x	x	✓	✓	x	x	✓	x	✓	x	x	x	x
Skin Sensitisation	x	✓	x	x	x	x	x	x	x	x	x	x	✓	x	x	x	x	x	x
T.Pyiformis toxicity (log ug/L)	0.2	1.1	0.3	0.2	0.4	0.2	0.3	0.2	0.5	0.3	0.3	0.2	1.1	0.2	1.3	0.3	0.5	1.4	0.4
Minnow toxicity (log mM)	1.9	0.9	2.8	6.8	0.1	10.0	2.1	3.7	1.7	-0.2	2.3	4.0	-1.4	2.1	2.4	1.5	2.0	0.1	-0.6
Renal OCT2 substrate	x	x	x	x	✓	✓	x	x	x	x	x	x	x	x	x	x	x	x	x
AMES toxicity	x	x	x	x	x	x	x	x	x	✓	✓	✓	x	x	x	x	x	x	x

Table 4. Van der Waals energy, electrostatic and total energy of protein-ligand interaction.

Ligands	Van der waal energy	Electrostatic energy	Total interaction energy
Berberine	-15.3547	-75.2073	-90.562
Quercetin	-28.3759	-47.9282	-76.3041
Naringenin	-5.3146	-55.5276	-60.8422
Oxyberberine	-10.4676	-47.2335	-57.7011
Berlambine	-6.3236	-32.5844	-38.908
Aesculetin	-22.2502	-7.97232	-30.22252
Apoatropine	-16.9751	-6.65654	-23.6316
Coumarin	-10.1854	-1.95025	-12.13565
Liquiritin	-3.30278	-1.25229	-4.55507

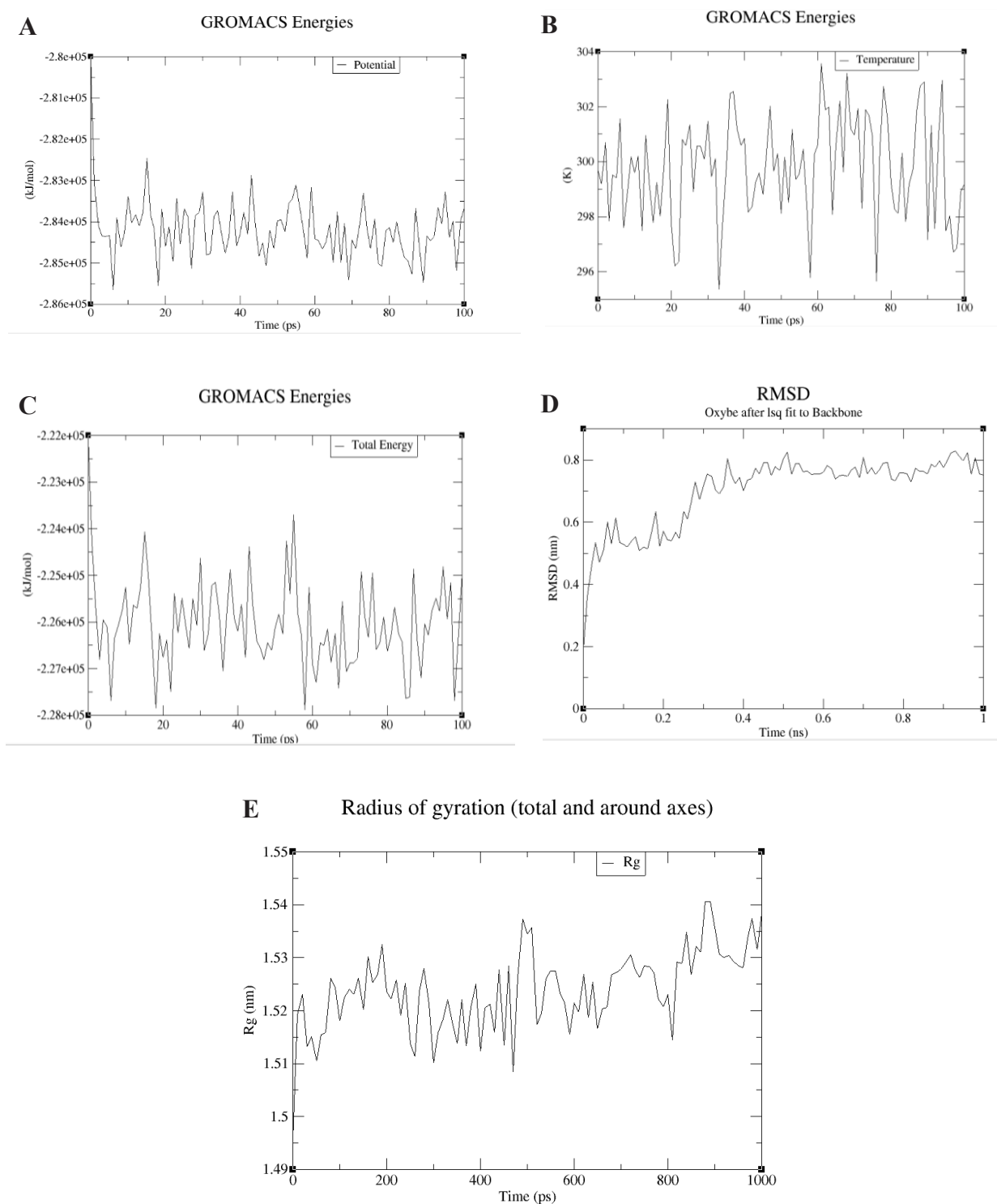


Figure 4. Fluctuations in **A:** Potential, **B:** Temperature, **C:** Total Energy, **D:** RMSD and **E:** Radius of gyration of protein during the simulation.

In this study, GROMACS—a widely used and efficient software for MD simulations—was employed to investigate molecular interactions at nanometer scales over picosecond to nanosecond timescales. The simulations confirmed that all evaluated protein-ligand complexes were stable, with interaction energy

values ranging from -4.55507 to -90.562 kcal/mol. Furthermore, MD simulations played a crucial role in identifying potential inhibitors of *Streptococcus pyogenes* Sortase C, a key bacterial enzyme absent in humans but essential for cell wall synthesis. Through a combination of protein sequence analysis, comparative

modeling, virtual screening, and molecular docking, three lead compounds (CID: 13888122, CID: 3694932, and CID: 102445430) were identified. MD simulations validated their stability and favorable binding free energies, reinforcing their potential as promising candidates for the development of inhibitors targeting Sortase C (Mangal *et al.*, 2023).

CONCLUSION

The results demonstrated that plants such as licorice, barberry, turmeric, plantain, nettle, cinnamon, aloe vera, and thyme contained the highest number of compounds with binding interactions ranging from -7.0 to -9.3 kcal/mol. In contrast, oregano, eucalyptus, sage, hyssop, and mangrove exhibited weaker interactions, with values between -6.0 and -7.0 kcal/mol.

Among the 19 tested compounds—methoxyhydrocarpine, linalyl acetate, kaempferol, glycyrrhizic acid, berlambin, tannin, naringenin, quercetin, amblyferon, berberine, askoltin, liquiritin, 1,3-disopropyl-naphthalene, ellagic acid, apotropin, coumarin, emodin, alpha-bourbonene, and carnosol—those derived from licorice, plantain, barberry, turmeric, nettle, cinnamon, aloe vera, and thyme exhibited the strongest binding energies with the transpeptidase enzyme.

Molecular dynamics (MD) simulations confirmed that the investigated complexes maintained sufficient stability throughout the simulation period. Moreover, the promising compounds showed favorable total interaction energy values, ranging from -4.55507 to -90.562 kcal/mol. These findings underscore the utility of the bioinformatics approach employed in this study, providing a solid foundation for subsequent experimental validation of the efficacy and safety of these compounds against bacterial targets. It is, however, essential to emphasize that experimental validation—either *in vivo* or *in vitro*—is critical for confirming these computational results and ensuring their practical applicability in future drug development efforts.

Conflict of interest

The authors indicate no conflict of interest in this work.

ACKNOWLEDGMENTS

The authors express their gratitude to Shahid Bahonar University of Kerman for providing the necessary facilities.

REFERENCES

- Ashraf M. V., Pant S., Khan M. H., Shah A. A., Siddiqui S., Jeridi M., and Ahmad S. (2023). Phytochemicals as antimicrobials: prospecting Himalayan medicinal plants as source of alternate medicine to combat antimicrobial resistance. *Pharmaceuticals*, 16(6): 881.
- Barh D., Tiwari S., Jain N., Ali A., Santos A. R., Misra A. N., and Kumar A. (2011). In silico subtractive genomics for target identification in human bacterial pathogens. *Drug Development Research*, 72(2): 162-177.
- Blundell T. L., Sibanda B. L., Montalvão R. W., Brewerton S., Chelliah V., Worth C. L., and Burke, D. (2006). Structural biology and bioinformatics in drug design: opportunities and challenges for target identification and lead discovery. *Philosophical Transactions of the Royal Society B: Biological Sciences*, 361(1467): 413-423.
- Borkotoky S., and Banerjee M. (2020). A computational prediction of SARS-CoV-2 structural protein inhibitors from *Azadirachta indica* (Neem). *Journal of Biomolecular Structure and Dynamics*, 39(11): 4111-4121.
- Carugo O., and Pongor S. (2001). A normalized root-mean-square distance for comparing protein three-dimensional structures. *Protein Science*, 10(7): 1470-1473.
- Groenhof G. (2013). Introduction to QM/MM simulations. In: Monticelli, L., Salonen, E. (Eds.), *Biomolecular simulations* (pp. 43-66), Methods in Molecular Biology, Vol. 924, Humana Press, Totowa, NJ. DOI: https://doi.org/10.1007/978-1-62703-017-5_3.
- Guilherme L., Kalil J., and Cunningham M. (2006). Molecular mimicry in the autoimmune pathogenesis of rheumatic heart disease. *Autoimmunity*, 39(1): 31-39.
- Hanwell M. D., Curtis, D. E., Lonie D. C., Vandermeersch T., Zurek, E., and Hutchison G. R. (2012). Avogadro: an advanced semantic chemical editor, visualization, and analysis platform. *Journal of Cheminformatics*, 4(1): 1-17.
- Hess B., Bekker H., Berendsen H. J., and Fraaije J. G. (1997). LINCS: a linear constraint solver for molecular simulations. *Journal of Computational Chemistry*, 18(12): 1463-1472.
- Hospital A., Goñi J. R., Orozco M., and Gelpí J. L. (2015). Molecular dynamics simulations: advances and applications. *Advances and Applications in Bioinformatics and Chemistry*, 8: 37-47. DOI: <https://doi.org/10.2147/aabc.s70333>.
- Islam M. T., Aktaruzzaman M., Saif A., Sourov M. M. H., Sikdar B., Rehman S., and Muhib M. M. A. (2024). Identification of acetylcholinesterase inhibitors from traditional medicinal plants for Alzheimer's disease using in silico and machine learning approaches. *RSC Advances*, 14(47): 34620-34636.
- Kadi R. H., Altammar K. A., Hassan M. M., Shater A. F., Saleh F. M., Gattan H., and Mohammedsaleh Z. M. (2022). Potential therapeutic candidates against Chlamydia pneumonia discovered and developed in silico using core proteomics and molecular docking and

- simulation-based approaches. *International Journal of Environmental Research and Public Health*, 19(12): 7306.
- Kang H. J., Coulibaly F., Proft T., and Baker E. N. (2011). Crystal structure of Spy0129, a *Streptococcus pyogenes* class B sortase involved in pilus assembly. *PloS One*, 6(1): e15969.
- Maheswari K. U., and Sankar S. (2024). In silico molecular docking of phytochemicals of *Murraya koenigii* against *Streptococcus mutans*. *Cureus*, 16(2): e53679. DOI: <https://doi.org/10.7759/cureus.53679>.
- Mangal P., Jha R. K., Jain M., Singh A. K., and Muthukumar J. (2023). Identification and prioritization of promising lead molecules from *Syzygium aromaticum* against Sortase C from *Streptococcus pyogenes*: an in silico investigation. *Journal of Biomolecular Structure and Dynamics*, 41(12): 5418-5435.
- Melk M. M., and El-Sayed A. F. (2024). Phytochemical profiling, antiviral activities, molecular docking, and dynamic simulations of selected *Ruellia* species extracts. *Scientific Reports*, 14(1): 15381.
- Morris G. M., Huey R., Lindstrom W., Sanner M. F., Belew R. K., Goodsell D. S., and Olson A. J. (2009). AutoDock4 and AutoDockTools4: Automated docking with selective receptor flexibility. *Journal of Computational Chemistry*, 30(16): 2785-2791.
- Nair P. C., and Miners J. O. (2014). Molecular dynamics simulations: from structure function relationships to drug discovery. *In Silico Pharmacology*, 2: 1-4.
- Pettersen E. F., Goddard T. D., Huang C. C., Couch G. S., Greenblatt D. M., Meng E. C., and Ferrin T. E. (2004). UCSF Chimera—a visualization system for exploratory research and analysis. *Journal of Computational Chemistry*, 25(13): 1605-1612.
- Piard J., Hautefort I., Fischetti V., Ehrlich S., Fons M., and Gruss A. (1997). Cell wall anchoring of the *Streptococcus pyogenes* M6 protein in various lactic acid bacteria. *Journal of Bacteriology*, 179(9): 3068-3072.
- Rehman A., Wang X., Ahmad S., Shahid F., et al. (2021). In silico core proteomics and molecular docking approaches for the identification of novel inhibitors against *Streptococcus pyogenes*. *International Journal of Environmental Research and Public Health*, 18(21): 11355.
- Shakeran Z., and Nosrati M. (2019). Bioinformatics study of the effects of some phytochemicals found in *Ferulago angulat*, *Scrophularia striata* and *Laurus nobilis* medicinal plants on inhibition of the proteins causing antibiotic resistance in *Staphylococcus aureus*: a descriptive study. *Journal of Rafsanjan University of Medical Sciences*, 18(2): 177-192.
- Thomford N. E., Senthebane D. A., Rowe A., Munro D., Seele P., Maroyi A., and Dzobo K. (2018). Natural products for drug discovery in the 21st century: innovations for novel drug discovery. *International Journal of Molecular Sciences*, 19(6): 1578.
- Trott O., and Olson A. J. (2010). AutoDock Vina: improving the speed and accuracy of docking with a new scoring function, efficient optimization, and multithreading. *Journal of Computational Chemistry*, 31(2): 455-461.
- Yırtıcı Ü., Ergene A., Atalar M. N., and Adem Ş. (2022). Phytochemical composition, antioxidant, enzyme inhibition, antimicrobial effects, and molecular docking studies of *Centaurea sivasica*. *South African Journal of Botany*, 144: 58-71.